



## SURFACE SCIENCE LETTERS

### STRUCTURE DETERMINATION OF THE RECONSTRUCTED Au(110) SURFACE

W. MORITZ and D. WOLF

*Institut für Kristallographie und Mineralogie der Universität München, Theresienstrasse 41,  
D-8000 München 2, Fed. Rep. Germany*

Received 12 June 1979; accepted for publication 10 August 1979

The LEED pattern of the Au(110) surface shows a  $(1 \times 2)$  and also a  $(1 \times 3)$  superstructure. The  $(1 \times 2)$  superstructure has been determined by comparison of LEED intensities with model calculations. The missing row model is the most probable model. A minimum of the averaged  $\bar{r}$ -factor,  $\bar{r} = 0.36$ , has been found for 15% contraction of the first layer spacing without atomic displacements in the second layer.

The clean (110) faces of gold are known to exhibit a reconstruction of the atomic arrangement in the surface layers with respect to the bulk structure. Until now a  $(1 \times 2)$  superstructure with a doubling of the lattice spacing in [001] direction has been reported [1,2]; now also a  $(1 \times 3)$  superstructure has been found. Characteristic for both structures are diffuse LEED beams, significantly broadened in [001] direction. The angular half width of the beams depends on energy and angle of incidence. This behaviour has been interpreted previously for the  $(1 \times 2)$  superstructure, applying a disordered missing row model with a slightly roughened surface [2,3]. This model can be used as well to explain the existence of the  $(1 \times 3)$  superstructure. Similar superstructures have been observed at the (110) faces of platinum and iridium [4] and a first structure analysis by LEED for Ir (110)- $(1 \times 2)$  [5] shows, that the missing row model is the most probable one. Here we present a LEED structure determination, assuming a well-ordered superstructure, neglecting the effect of the disorder of the (110) surface.

The Au crystal of 5N purity has been oriented within  $0.5^\circ$  of the [110] direction by X-ray diffraction and was cut and planed by spark erosion. Electrochemical etching in 5N  $H_2SO_4$  followed by electrolytical polishing in a cyanide solution produced a smooth reflecting surface. After argon ion bombardment the LEED pattern exhibits a very diffuse  $(1 \times 2)$  superstructure – fig. 1a – which coalesces after tempering up to 800 K into the pattern of a  $(1 \times 2)$  or  $(1 \times 3)$  structure.

The conditions at which the  $(1 \times 3)$  superstructure appears are not quite clear; it seems to be dependent on the special ion bombardment conditions and probably on the cooling rate after tempering. In both cases the spots are broadened in [001] \*

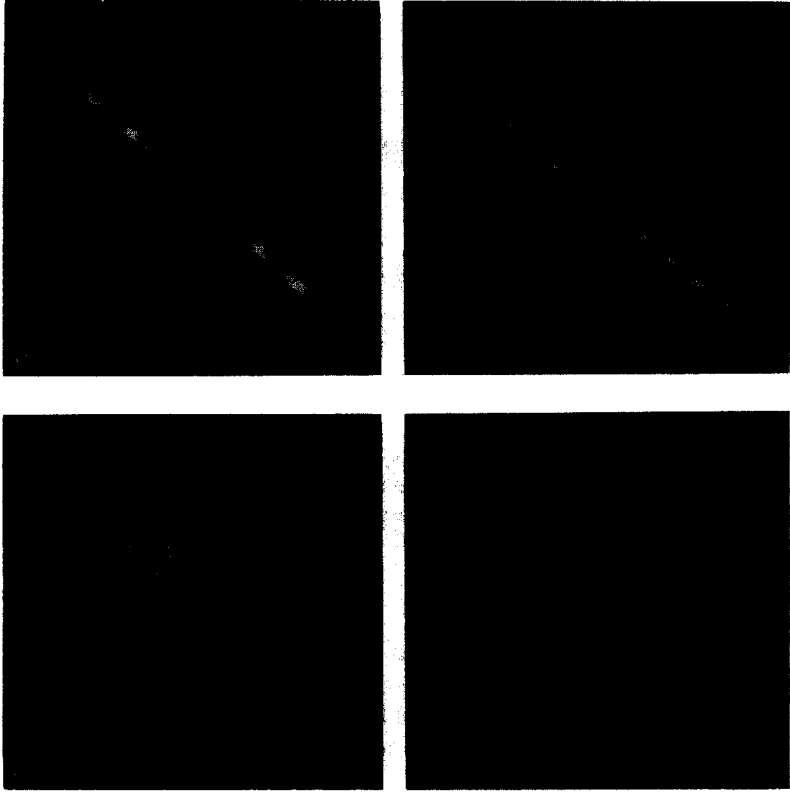


Fig. 1. Diffraction pattern of the Au(110) surface,  $E_p = 48$  eV: (a) diffuse spots after ion bombardment,  $T = 300$  K; (b)  $(1 \times 3)$  superstructure,  $T = 300$  K; (c)  $(1 \times 2)$  superstructure,  $T = 300$  K; (d)  $(1 \times 1)$  structure,  $T = 750$  K.

direction — figs. 1b and 1c. The superstructures cannot be caused by adatoms since no impurities could be detected by Auger electron spectroscopy. The  $(1 \times 3)$  structure is stable up to 350 K. Above this temperature an irreversible transition to the  $(1 \times 2)$  structure is found, which is stable up to 670 K. Above 670 K a rapid decrease of the integral intensity of the half order beams, correlated with broadening of the angular intensity profile is observed. At 720 K only integer order beams can be seen visually on the screen — fig. 1d. A detailed study of the thermal stability of the superstructures and the transitions  $(1 \times 3) \rightarrow (1 \times 2) \rightarrow (1 \times 1)$  will be published. The following structure analysis only deals with the  $(1 \times 2)$  superstructure.

Nineteen LEED intensity—voltage spectra at normal incidence — 11 integer order and 8 half order beams — have been measured, using a special LEED diffractometer, consisting of a movable electron gun [3] and a computer-controlled Fara-

day cup. For integral intensity measurements the diffracted beams have been collected with a detector of  $4^\circ$  aperture. All beams have been remeasured several times after ion bombardments and annealing, achieving in this way highly reproducible beam measurements.

Intensity calculations have been done for the missing row model – fig. 2a – a modification of the missing row model including small displacements in the second layer – fig. 2b – and a row-pairing model – fig. 2c. Two further models could be possible: a distorted hexagonal top-most layer as has been proposed recently [6] and an up-down row model.

Model calculations for the first of the latter two models have not yet been done; the first results for the second model show this model to be most unlikely. A detailed  $r$ -factor analysis for the up-down row model has been omitted since only poor correspondence could be found between experimental and theoretical curves by visual comparison.

The calculations were performed using the RFS-scheme and the layer-doubling method [7]. Up to eight phase shifts have been included and up to sixty symmetrically nonequivalent beams have been used. The phase shifts resulted from a relativistic band structure potential and were spin-averaged [8], the inner potential

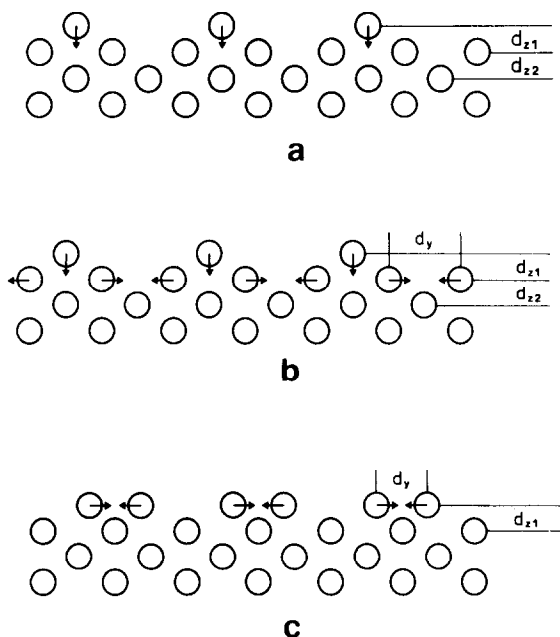


Fig. 2. Side views of surface models: (a) missing row model; (b) missing row model with additional displacement in the second layer; (c) row-pairing model. The  $z$ -direction is perpendicular to the crystal surface,  $x$ - and  $y$ -directions are in the surface plane.

related to this set of phase shifts has been found to be  $V_0 = 9$  eV. All calculations have been done with a bulk Debye temperature  $T_D = 170$  K [9], and a damping constant varying between 4 and 6 eV. The best agreement of theoretical and experimental curves is reached for 5 eV. Some examples of measured and calculated intensity–voltage spectra are shown in Fig. 3.

The agreement between theory and experiment has been determined quantitatively by the  $r$ -factor analysis, using the computer program developed by Zanazzi and Jona [10]. Some  $r$ -factor curves for the missing row model are displayed in fig. 4. A significant minimum is existent for 15% contraction of the first layer spacing, that is a distance  $d_{z1} = 1.225$  Å compared to the bulk value of  $d_{zb} = 1.442$  Å, the variation having been done in steps of  $\Delta d_{z1} = 0.036$  Å, which is 2.5% of the bulk distance. The results indicate that there are none or only small displacements within the second layer. As can be estimated from fig. 4, a  $d_z$ -shift of the atoms within the second layer must be smaller than  $\Delta d_{z2} = \pm 0.05$  Å. Also all displacements in the  $y$ -direction in the second layer, ranging from  $d_{y2} = 3.88$  Å to  $d_{y2} = 2.86$  Å, which is

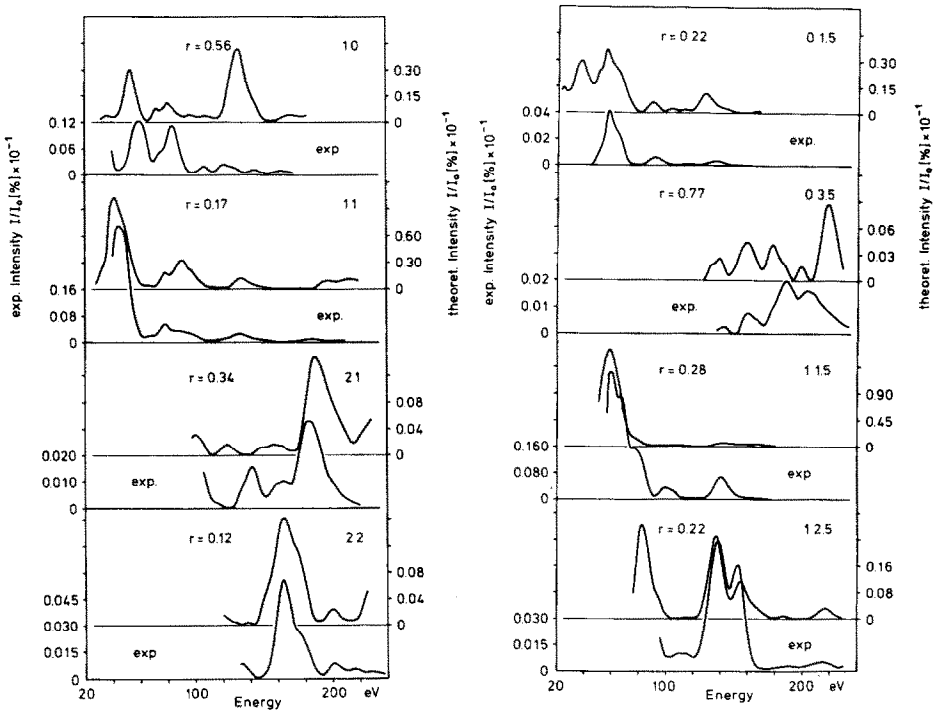


Fig. 3. Experimental and theoretical LEED spectra for normal incidence. The calculated spectra corresponds to the missing row model with 15% contraction of the first layer spacing. The  $r$ -factors are given.

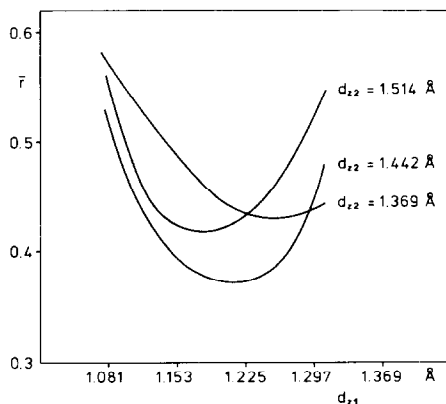


Fig. 4. Mean reliability factor  $\bar{r}$  for the missing row model as a function of the first and second layer spacing  $d_{z1}$  and  $d_{z2}$ ;  $\bar{r}_{\min} = 0.36$ .

a variation of the bulk value  $d_{yb} = 4.08 \text{ \AA}$  between  $-5\%$  and  $-30\%$ , produced increasing  $r$ -factors; possible displacements must be smaller than  $\Delta d_y = 0.1 \text{ \AA}$ .

The averaged  $r$ -factor for the row-pairing model, calculated for all lateral chain distances between  $d_y = 4.08 \text{ \AA}$  and  $d_y = 2.8 \text{ \AA}$  in steps of  $\Delta d_y = 0.2 \text{ \AA}$ , is always greater than  $\bar{r} = 0.5$ ; this result cannot be improved by variation of a second parameter, the first layer spacing  $d_{z1}$ , between  $d_{z1} = 1.5 \text{ \AA}$  and  $d_{z1} = 1.2 \text{ \AA}$ .

For the missing row model the minimum of the averaged  $r$ -factor calculated for 19 beams is  $\bar{r} = 0.36$  with a structure  $R$ -factor [10] of  $R = 0.28$ . For some beams the experimental intensity spectra are found to agree well with the calculated profiles, equivalent to  $r \leq 0.15$ , while some other beams show only a poor correspondence with the experiment ( $r \geq 0.5$ ). This is especially the case with the (10) and the (03.5) beam. Nevertheless, no other model calculation produced a lower  $r$ -factor for these two beams. The misfit which is still present may have two reasons: first, the inner potential and the damping constant have been assumed to be independent from energy, and the temperature factor has been set equal for all layers; second, the disorder of the surface has been neglected. Though the averaged  $r$ -factor  $\bar{r} = 0.36$  is relatively high, we conclude that the missing row model with a contraction of the first layer spacing of  $15\%$  is the most probable model.

Grateful acknowledgement is made to the Deutsche Forschungsgemeinschaft — Sonderforschungsbereich 128 — for financial support. We thank Dr. M. Van Hove for helpful discussions and supplying the layer-doubling program. We are grateful to Mr. H. Plöckl and Mr. J. Csiszar for technical assistance.

**References**

- [1] D.G. Fedak and N.A. Gjostein, *Acta Met.* 15 (1967) 827.
- [2] D. Wolf, Dissertation, Universität München (1972).
- [3] D. Wolf, H. Jagodzinski and W. Moritz, *Surface Sci.* 77 (1978) 265.  
D. Wolf, H. Jagodzinski and W. Moritz, *Surface Sci.* 77 (1978) 283.
- [4] K. Christmann and G. Ertl, *Z. Naturforsch.* 28a (1973) 1144;  
H.P. Bonzel and R. Ku, *J. Vacuum Sci. Technol.* 9 (1972) 663.
- [5] C.-M. Chan, M.A. Van Hove, W.H. Weinberg and E.D. Williams, *Solid State Commun.* 30 (1979) 47.
- [6] E. Lang, K. Heinz and K. Müller, *Verh. Deut. Physik. Ges.* 1 (1979) 278.
- [7] J.B. Pendry, *Low Energy Electron Diffraction* (Academic Press, London, 1974).
- [8] R. Feder and W. Moritz, *Surface Sci.* 77 (1978) 505.
- [9] *International Tables for X-Ray Crystallography*, Vol. III.
- [10] E. Zanazzi and F. Jona, *Surface Sci.* 62 (1977) 61.